

# Naive parton picture for color transparency of kaon in the electronuclear reaction $A(e, e'K^+)$

Kook-Jin Kong

*Research Institute of Basic Science, Korea Aerospace University, Goyang 10540, Korea*

Tae Keun Choi

*Department of Physics and Engineering Physics, Yonsei University, Wonju 26493, Korea*

Byung-Geel Yu\*

*Research Institute of Basic Science, Korea Aerospace University Goyang, 10540, Korea*

Nuclear transparency in the kaon-induced nuclear reaction  $A(e, e'K^+)$  is investigated in parallel with our previous study on the pion transparency in Phys. Rev. C **111**, 064608 (2025). Based on the Glauber scattering theory, which incorporates shadowing by the two-step process, the kaon color transparency (CT) is analyzed to find that the slope of the kaon CT steeper than the pion CT along with the photon virtuality  $Q^2$  increase is well accounted for by the naive parton model (NPM) rather than by the quantum diffusion model (QDM). Further diminishing of CT due to shadowing in the initial state yields better agreement with experimental data. The dependence of kaon transparency on  $Q^2$  up to 10 GeV<sup>2</sup>/c<sup>2</sup> and the mass number  $A$  is presented for comparison with the JLab data at the 6 GeV electron beam for the reaction  $A(e, e'K^+)$  in <sup>12</sup>C, <sup>63</sup>Cu, and <sup>197</sup>Au nuclei.

PACS numbers: 11.80.La, 24.85.+p, 25.30.Rw, 13.60.Le, 25.80.Nv

Keywords:

## I. INTRODUCTION

Nuclear transparency is an interesting topic that provides a testing ground for the onset of CT [1–3], as predicted by quantum chromodynamics (QCD) in various nuclear reactions. According to QCD, the nuclear transparency should increase with  $Q^2$  due to the suppression of color interaction by the  $q\bar{q}$  structure of the produced meson, forming a color singlet small-size configuration (SSC). At high virtualities, this is because the transverse size of SSC contracts, proportional to the virtual photon momentum  $1/\sqrt{Q^2}$ , which renders the color field of the color dipole moment from the  $q\bar{q}$  structure vanishing. Color transparencies of electronuclear reactions induced by virtual photons, such as  $A(e, e'\pi^+)$  and  $A(e, e'\rho^0)$ , have been investigated theoretically [4–11] and experimentally [12–15].

However, in contrast to such an extensive study of color transparency in the isospin sector, research into this issue in the strangeness sector has been rare in both theory and experiment. Only recently is the kaon transparency from the reaction  $A(e, e'K^+)$  reported to have been measured at JLab using the 6 GeV electron beam [16], with the relevant theoretical analysis found in Ref. [17], which incorporates the QDM in the Glauber scattering theory. On the theoretical side, investigating the onset of kaon CT in nuclei is interesting because it occurs via the intranuclear kaon-nucleon interaction with the subnuclear process related to the strangeness production from the

proton sea and the gluon contributions in the microscopic picture.

An introduction to kaon-nucleon/nucleus interaction with a brief review of the relevant issues can be found in Ref. [17]. Consequently, such a different production mechanism from the isospin flavor manifests itself via  $KN$  scattering at the level of hadronic degrees of freedom, which is weaker than  $\pi N$  scattering, thus, revealing a higher transparency. Indeed, the recent JLab experiment on the reaction  $A(e, e'K^+)$  shows an increase in the kaon CT with respect to  $Q^2$  steeper than the pion CT, as expected for the aforementioned reason. Nevertheless, the current Glauber approach to this reaction using QDM likely has difficulty reproducing the steep rise of the kaon CT along with  $Q^2$ , in particular [17], unlike the pion CT in the  $A(e, e'\pi^+)$  reaction, which is well reproduced by the QDM applied to the Glauber theory (GT) [4]. Furthermore, the choice of the value for  $\Delta M^2$ , which should be a crucial ingredient in QDM, has a weak physical background on its difference from the value for the pion case.

In this paper, we will explore the possibility of microscopic models other than QDM for a better description of the  $Q^2$  dependence of the kaon CT in the  $A(e, e'K^+)$  reaction, as reported in Ref. [16]. This paper is organized as follows. Section II discusses formulations of NPM in addition to QDM to analyze the  $Q^2$  dependence of kaon transparency in the  $A(e, e'K^+)$  reaction, based on our previous work in Ref. [4] for pion electronuclear reaction  $A(e, e'\pi^+)$ . The shadowing effect introduced in our previous work [4] will be included as another absorption mechanism that diminishes the kaon CT. The kaon transparency is reproduced, including the ratio normalized by

---

\*bgyu@kau.ac.kr

TABLE I: Kinematical variables  $Q^2$  ( $\text{GeV}^2/c^2$ ),  $W$  (GeV),  $E_e$  (GeV),  $\theta_e$  (deg),  $E_{e'}$  (GeV),  $x_B$ , and  $|\mathbf{p}_K|$  (GeV/c) in kaon electroproduction and relevant quantities to the experiment at JLab [16] for kaon transparency in the range of  $0.5 \leq Q^2 \leq 10 \text{ GeV}^2/c^2$ . The coherent length  $l_c$  (fm) with mass  $m_\phi$  in Eq. (2) and the formation lengths,  $l_f^{\text{NPM}}$  with  $R_K = 0.58 \text{ fm}$  in Eq. (3) and  $l_f^{\text{QDM}}$  (fm) with  $\Delta M^2 = 0.3 \text{ GeV}^2$  chosen in Eq. (4) are displayed. The total cross section  $\sigma_{KN}$  (mb) in the last column is chosen from the particle data group (PDG) less dependent on the kaon momentum  $p_K$  [GeV/c] in the given range [18]. We use  $\sigma_{\phi N} = 18 \text{ mb}$  for the calculation of the shadowing by the two-step process [4].

$Q^2$	$W$	$E_e$	$\theta_e$	$E_{e'}$	$x_B$	$ \mathbf{p}_K $	$l_c$	$l_f^{\text{NPM}}$	$l_f^{\text{QDM}}$	$\sigma_{KN}$
0.55	2.28	3.4	26	0.8	0.11	2.24	0.65	2.7	2.95	
0.69	2.25	3.5	27	0.9	0.14	2.22	0.60	2.68	2.93	
0.77	2.25	3.68	26	1.04	0.16	2.26	0.58	2.71	2.97	18
0.92	2.26	3.85	27	1.1	0.18	2.36	0.56	2.83	3.10	
1.05	2.26	4.02	27	1.2	0.2	2.41	0.54	2.89	3.17	
1.10	2.26	4.02	27.76	1.19	0.21	2.42	0.53	2.9	3.18	
2.15	2.21	5.01	28.85	1.73	0.35	2.74	0.41	3.27	3.60	
3.0	2.14	5.01	37.77	1.43	0.45	2.89	0.35	3.45	3.81	17
3.91	2.26	5.77	40.38	1.42	0.48	3.61	0.35	4.29	4.76	
4.69	2.25	5.77	52.67	1.03	0.53	3.90	0.33	4.62	5.14	
5.0	2.43	11.0	16.28	5.67	0.5	4.57	0.35	5.4	6.00	
6.5	2.74	11.0	22.13	4.01	0.5	6.25	0.37	7.37	8.23	18
8.0	3.02	11.0	32.37	2.34	0.49	7.94	0.38	9.34	10.44	
9.5	3.09	11.0	47.71	1.32	0.52	8.89	0.36	10.46	11.69	

the transparency of  $^{12}\text{C}$  and the transparency depending on the mass number  $A$ . These results will then be compared with the JLab data at the 6 GeV electron beam. A summary and conclusion will follow in the final section.

## II. MODELS FOR DATA ANALYSIS

The reaction  $A(e, e' K^+)$  is induced by the subnuclear process  $\gamma^*(k) + p(p) \rightarrow K^+(p_K)\Lambda(p')$  (or  $\Sigma^0$ ) with the kinematical quantities relevant to the process listed in Table I. The GT for the kaon transparency  $T_A$  which includes the shadowing effect by the two-step process in the  $A(e, e' K^+)$  reaction is written as [4]

$$T_A = \frac{1}{A} \int_0^\infty d^2b \int_{-\infty}^\infty dz \varrho(\mathbf{b}, z) \times \exp \left[ - \int_{z-l_c}^z \sigma_{\phi N} \varrho(\mathbf{b}, z') dz' - \int_z^\infty \sigma_{KN}^{\text{eff}}(z') \varrho^*(\mathbf{b}, z') dz' \right] \quad (1)$$

where  $\varrho$  and  $\varrho^*$  are the nuclear density function for the nucleus of  $A$  and for the recoiled nuclear state  $A-1$  with the kaon produced. We use the Wood-Saxon distribution for the density function in the present work with the diffusion parameter  $d = \sqrt{3}/\pi$  [4]. Expressing  $T_A$  in the order of the reaction process, the first term corresponds

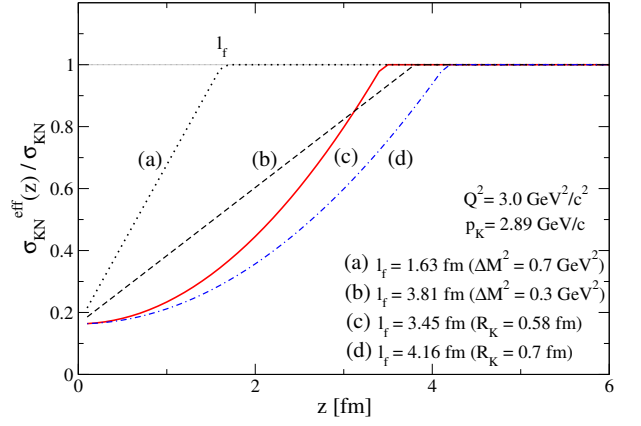


FIG. 1: Ratio of the cross section  $\sigma_{KN}^{\text{eff}}/\sigma_{KN}$  in Eq (5) vs distance  $z$  at  $Q^2 = 3.0 \text{ GeV}^2/c^2$  and  $p_K = 2.89 \text{ GeV}/c$ . The quadratic increase by NPM and linear one by QDM are shown with the formation length  $l_f$  estimated by Eqs. (3) and (4).

to the shadowing by the two-step process in the initial state where the fluctuation of virtual photon into a vector meson occurs at the position  $z - l_c$  [19–21], and then a kaon is produced at  $z$  to scatter off a nucleon via the cross section  $\sigma_{KN}$  in the second term to undergo the attenuation on its way out to a nucleus. Since the virtual photon  $\gamma^*$  fluctuates into  $\phi(1020)$  vector via  $\phi(1020) \rightarrow K^+ K^-$ , the coherent length due to the  $\phi$  coupling to kaon is given by

$$l_c = 2\nu/(Q^2 + m_\phi^2), \quad (2)$$

and listed in Table I in accordance with the  $Q^2$  values.

In the present framework, determining the cross section for  $KN$  scattering is crucial to evaluating the  $Q^2$  dependence of the QDM or NPM of the produced kaon through the kaon-nucleus optical potential. The size of the cross section  $\sigma_{\phi N}$  is also requisite to evaluate the contribution of shadowing. The  $\phi N$  scattering cross section is indirectly determined via photoproduction data and nuclear transparency measurements, with free space estimates around  $10 \simeq 20 \text{ mb}$  [22–24]. We use the value of  $\sigma_{KN}$  read from the PDG, as listed in Table I, while the value of  $\sigma_{\phi N} = 18 \text{ mb}$  is taken, following Ref. [25].

To implement CT in the GT, a microscopic model such as the QDM is introduced the validity of which has been proven for both the pion CT and the  $\rho^0$  CT [13, 26–28]. However, the QDM applied to the kaon CT observed in the JLab data does not appear to reproduce its slope as the increasing  $Q^2$  to a good degree, even when the mass parameter  $\Delta M^2$  in the formation length is refitted to the data, as discussed in Ref. [17].

For a better improvement, we investigate the possibility of the naive parton model (NPM) in addition to the QDM prediction in the GT. We trace the  $Q^2$  dependence of  $T_A$  on a more general basis. In Ref. [29], the effective cross section for  $KN$  scattering and its expansion through the formation length  $l_f$  are discussed in the naive parton picture and quantum diffusion model, where

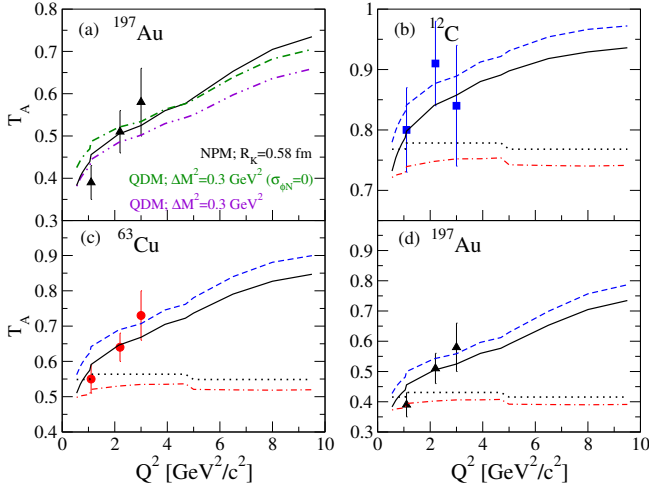


FIG. 2:  $Q^2$  dependence of the nuclear transparency  $T_A$  in  $^{12}\text{C}$ ,  $^{63}\text{Cu}$ , and  $^{197}\text{Au}$  nuclei. The solid curve shows the kaon CT calculated in the GT in Eq. (1), where NPM with  $R_K = 0.58$  fm is used and the shadowing effect is evaluated using  $\sigma_{\phi N} = 18$  mb. The dashed curve is from NPM without shadowing. The dotted curve is from the pure GT, which includes neither NPM nor shadowing in Eq. (1). The dash-dotted curve depicts the contribution of shadowing in the pure GT. For comparison with the result of NPM in the  $^{197}\text{Au}$  nucleus, the prediction from QDM with  $\Delta M^2 = 0.3$   $\text{GeV}^2$  is presented in (a), where the dash-dot-dotted and dash-dash-dotted curve denote  $T_A$  with and without shadowing, respectively. Data are taken from Ref. [16].

the size of the cross section is estimated from the relation  $\sigma_{KN}^{\text{eff}}/\sigma_{KN} \simeq x_t^2/\langle x_t^2 \rangle \simeq \langle k_t^2 \rangle/Q^2$  by using the uncertainty principle with  $n$  multiplied for the quark number. Meanwhile, partons separating at the velocity  $c$  travel the longitudinal coordinate  $z \sim (E/m)x_t$ , which is called a formation length with the relativistic correction. This can be written as

$$l_f^{\text{NPM}} = \left( \frac{E_K}{m_K} \right) R_K, \quad (3)$$

where the transverse size of a hadron is replaced by the charge radius in this work for practical purpose. In contrast, the formation length of QDM expands during the time  $\Delta t = 1/\Delta E$  by the uncertainty in the energy of the final kaonic states [8], giving

$$l_f^{\text{QDM}} = \frac{2p_K}{\Delta M^2}. \quad (4)$$

The effective cross section that embraces both models is written as

$$\sigma_{KN}^{\text{eff}}(z) = \sigma_{KN} \left[ \theta(z - l_f) + \left\{ \frac{n^2 \langle k_t^2 \rangle}{Q^2} \left( 1 - \left( \frac{z}{l_f} \right)^\tau \right) + \left( \frac{z}{l_f} \right)^\tau \right\} \theta(l_f - z) \right], \quad (5)$$

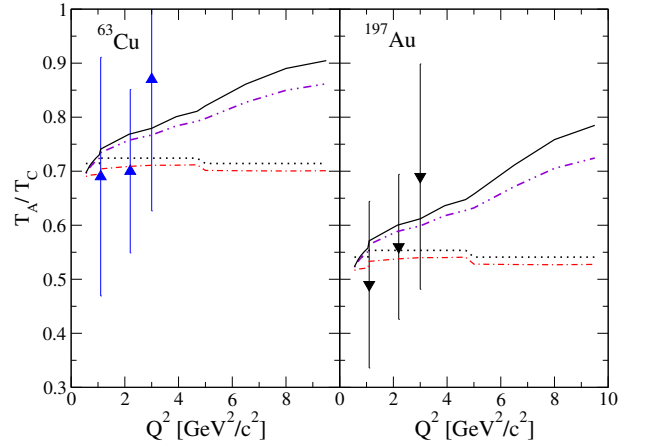


FIG. 3:  $Q^2$  dependence of the ratio of  $T_A$  normalized by the  $T_A$  of  $^{12}\text{C}$  from NPM. The solid curve represents the ratio  $T_A/T_C$  from the GT+shadowing+NPM with the notation for the curve the same as in Fig. 2. The dash-dot-dotted curve shows the  $T_A/T_C$  from the GT+shadowing+QDM with  $\Delta M^2 = 0.3$   $\text{GeV}^2$ . Data are taken from Ref. [16].

where the case of  $\tau = 2$  leads to the NPM, and  $\tau = 1$  to the QDM estimation of the CT with the respective formation lengths in Eqs. (3) and (4) discussed above. The transverse momentum of the quark/antiquark in the kaon is chosen to be  $\langle k_t^2 \rangle^{1/2} \simeq 0.35$   $\text{GeV}^2$ . The cross section  $\sigma_{KN}$ , originally a function of kaon momentum, is now to be constant as listed in Table I, because it varies very slowly without resonances in the momentum region of interest in the  $K^+p$  scattering [18].

In the NPM calculation, we use the kaon radius  $R_K = 0.58$  fm in Eq. (3) from the mean square charge radius,  $\langle R_K^2 \rangle = 0.34 \pm 0.05$   $\text{fm}^2$  measured in experiments [30]. The mass-squared parameter  $\Delta M^2$  in Eq. (4) is applied to the QDM estimation of the kaon CT, with the value 0.3  $\text{GeV}^2$  advocated in Ref. [17], while for an agreement with the pion CT, the value of 0.7  $\text{GeV}^2$  is favored in various model calculations.

In Fig. 1 we present the ratio of the cross section  $\sigma_{KN}^{\text{eff}}/\sigma_{KN}$  in Eq. (5) to compare the  $z$ -dependence of NPM with QDM at  $Q^2 = 3$   $\text{GeV}^2/c^2$  and  $p_K = 2.89$   $\text{GeV}/c$ . The dotted, dashed, solid, and dash-dotted curves correspond to the formation length of  $l_f = 1.63$  fm with  $\Delta M^2 = 0.7$   $\text{GeV}^2$  and 3.81 fm with  $\Delta M^2 = 0.3$   $\text{GeV}^2$  from QDM, and  $l_f = 3.45$  fm with  $R_K = 0.58$  fm and  $l_f = 4.16$  fm with  $R_K = 0.7$  fm from NPM, demonstrating a linear and a quadratic contribution, respectively, in accordance with the powers of  $z/l_f$ . As shown, the contribution from the choice of  $\Delta M^2 = 0.7$   $\text{GeV}^2$  is half the smaller than others. In this work we choose the cases of  $\Delta M^2 = 0.3$   $\text{GeV}^2$  for QDM and  $R_K = 0.58$  fm for NPM to describe the CT in kaon electronuclear reaction.

Figure 2 shows the dependence of the kaon transparency  $T_A$  on the photon virtuality  $Q^2$  in three different nuclei,  $^{12}\text{C}$ ,  $^{63}\text{Cu}$ , and  $^{197}\text{Au}$ . Predictions are made us-

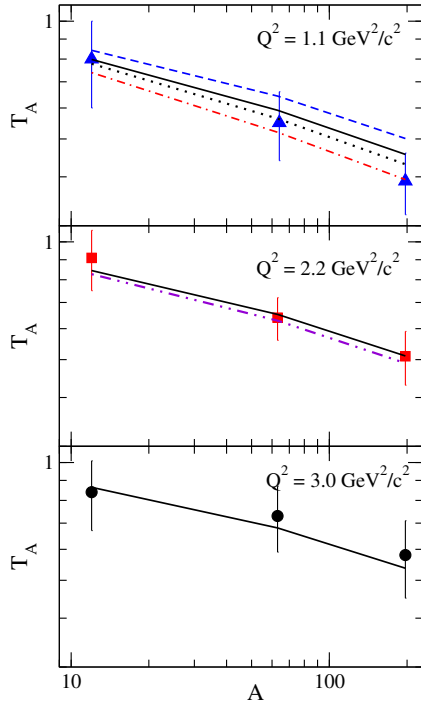


FIG. 4:  $A$  dependence of  $T_A$  at fixed  $Q^2$ . Solid and dashed curves correspond to the cases with and without shadowing at  $Q^2 = 1.1 \text{ GeV}^2/c^2$ , where other notations for the curves are the same as in Fig. 2. The QDM prediction is depicted by the dash-dot-dotted curve at  $Q^2 = 2.2 \text{ GeV}^2/c^2$  for comparison. Data are taken from Ref. [16].

ing the GT in Eq. (1) with the NPM in the final state for CT in Eq. (3), in addition to the shadowing by the two-step process in the initial state, and similarly for the case of QDM in Eq. (4). Given the total cross sections  $\sigma_{\phi N}$  and  $\sigma_{KN}$  as discussed above, we choose the  $T_A$  of the  $^{197}\text{Au}$  nucleus as an example of illustrating the difference in kaon CT between the QDM and NPM in panel (a). The solid curve represents the NPM prediction with  $R_K = 0.58 \text{ fm}$  chosen, together with the role of the shadowing in the initial state reducing the  $T_A$  further, as can be seen in other panels. In QDM, the widely accepted value of  $\Delta M^2 = 0.7 \text{ GeV}^2$  [4] is found to be invalid for reproducing the kaon CT, and thus, is excluded. However, the case of  $\Delta M^2 = 0.3 \text{ GeV}^2$  is comparable to the NPM prediction, if the initial shadowing is included (dash-dot-dotted curve). Though the choice of  $\Delta M^2$  in QDM could be different between the pion and kaon CTs as discussed above, it has less physical basis instead. In contrast, the NPM obtains agreement by using the kaon radius determined from experimental measurements. Furthermore, the steepness of the slope of the kaon CT is better reproduced by the quadratic increase of  $\sigma_{KN}^{\text{eff}}$  in NPM rather than by the linear one in QDM.

The ratio of the kaon transparency,  $T_A/T_C$ , normalized by the transparency of the  $^{12}\text{C}$  nucleus, is reconstructed from the JLab data [16] and analyzed in Fig. 3, while excluding the ratio of transparency over the deuteron

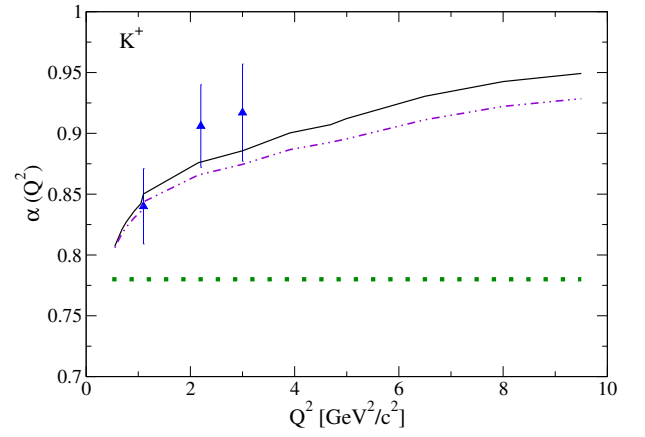


FIG. 5:  $Q^2$  dependence of  $\alpha$  for nuclear transparency  $T_A$ . The parameter  $\alpha$  is calculated by averaging over the three target nuclei. The result from QDM is presented by the dash-dot-dotted curve for comparison. The thick dotted line denotes the constant value for  $\alpha$  extracted from  $K^+$ -nucleus scattering [31]. Data are taken from Ref. [16].

because the GT is inadequate for such a non-spherical nuclear target with the small mass number. By definition in Eq. (1), the ratio of kaon CT has the advantage of reducing the nuclear effect due to the cancellation of the different nuclear density functions between the numerator and denominator.

The dependence of  $T_A$  on the mass number  $A$  is investigated in various nuclei in Fig. 4, showing a rapid decrease as  $A$  increases. By comparing the solid and dashed curves, the effect of shadowing on the kaon transparency can be observed. The  $T_A$  of the dash-dot-dotted curve from QDM is presented in the lowest panel for comparison.

An interesting issue related to the  $A$  dependence of  $T_A$  in Fig. 4 is tracing the  $Q^2$  dependence of the parameter  $\alpha$  by rewriting

$$T_A = A^{\alpha(Q^2)-1}, \quad (6)$$

where  $\sigma_A = A^\alpha \sigma_N$  is assumed for the nuclear cross section versus the nucleon cross section. Therefore, the deviation of  $\alpha$  from unity suggests a nuclear effect differing from the  $A$  nucleons in free space. The determination of  $\alpha(Q^2)$  by the  $\chi^2$ -fit was presented for  $\pi$  CT in Ref. [13], and the case of kaon CT was discussed in Ref. [16]. Following Ref. [16], the numerical consequence from  $T_A = (A/2)^{\alpha-1}$  is shown in Fig. 5, where the increase in  $\alpha$  is predicted by NPM for the experimental data in Ref. [16]. The bold dotted curve illustrates the constancy of  $\alpha$  obtained from hadron-nucleus scattering [31]. Unlike in hadron-nucleus scattering, where it remains almost constant at around 0.78 [31], the  $\alpha$  has a noticeable dependence on  $Q^2$ , up to 0.95, in electron-nucleus reactions,  $A(e, e'K^+)$ , and hence, confirming the volume effect by the electromagnetic probe rather than the surface-dominated contribution by the hadronic probe.

### III. CONCLUSION

We have studied the nuclear reaction  $A(e, e'K^+)$  in lighter and heavier nuclei,  $^{12}\text{C}$ ,  $^{63}\text{Cu}$ , and  $^{197}\text{Au}$ , to analyze the onset of kaon CT. Within the framework of GT in the range of  $0.55 \leq Q^2 \leq 10 \text{ GeV}^2/c^2$ , with shadowing by the two-step process in the initial state considered, we incorporated the QDM as well as the NPM to describe the kaon CT measured at the JLab 6 GeV electron beam. Unlike the case with pion transparency, under similar kinematical circumstances, the production of strangeness in the nucleon is less probable than that of isospin. This leads to the cross section for  $KN$  scattering being smaller than the  $\pi N$  scattering at the hadronic level, which, in turn, yields the kaon CT more transparent than the pion case. In this case, QDM, with the mass-squared parameter fixed to the pion CT, is insufficient to account for the kaon CT. In this work, we take advantage of the NPM over the QDM in explaining the higher kaon CT by the quadratic variation of the scattering cross section  $\sigma_{KN}$  during the formation length  $l_f$ . Based on the Glauber scattering theory, with shadowing considered in the initial state, we demonstrate that the NPM in the final state is suitable for investigating the onset of CT in reactions that involve strangeness production in nuclei.

To summarize, the advantages of the naive parton model over the quantum diffusion model are elucidated in describing the kaon color transparency, which is higher than that of the pion. It is also shown that the former model is less model-dependent than the latter one when using the measured value of the kaon charge radius in experiments for this crucial variable  $l_f$ . In contrast, QDM relies solely on the variable  $\Delta M^2$ , which is adjusted to fit the experimental color transparency data.

### ACKNOWLEDGMENT

This work was supported by the Grant No. NRF-2022R1A2B5B01002307 from the National Research Foundation (NRF) of Korea.

### DATA AVAILABILITY

The data supporting this study's findings are available within the article.

- 
- [1] L. L. Frankfurt, G. A. Miller, and M. Strikman, *Ann. Rev. Nucl. Part. Sci.* **44**, 501 (1994).
  - [2] S. J. Brodsky and A. H. Mueller, *Phys. Lett. B* **206**, 685 (1988).
  - [3] P. Jain, B. Pire, J.P. Ralston, *Phys. Rept.* **271**, 67 (1996).
  - [4] T. K. Choi, K.-J. Kong, and B.-G. Yu, *Phys. Rev. C* **111**, 064608 (2025).
  - [5] A. Larson, G. A. Miller, and M. Strikman, *Phys. Rev. C* **74**, 018201 (2006).
  - [6] B. Kundu, J. Samuelsson, P. Jain, and J. P. Ralston, *Phys. Rev. D* **62**, 113009 (2000).
  - [7] S. Das, *Phys. Rev. C* **105**, 035204 (2022).
  - [8] D. Dutta, K. Hafidi, and M. Strikman, *Prog. Part. Nucl. Phys.* **69**, 1 (2013).
  - [9] W. Cosyn and J. Ryckebusch, *Phys. Rev. C* **87**, 064608 (2013).
  - [10] B. Z. Kopeliovich, J. Nemchick, N. N. Nikolaev, and B. G. Zakharov, *Phys. Lett. B* **324**, 469 (1994).
  - [11] B. Z. Kopeliovich, J. Nemchik, and I. Schmidt, *Phys. Rev. C* **76**, 015205 (2007).
  - [12] B. Clasie *et al.*, *Phys. Rev. Lett.* **99**, 242502 (2007).
  - [13] X. Qian *et al.*, *Phys. Rev. C* **81**, 055209 (2010).
  - [14] A. Airapetian *et al.*, *Phys. Rev. Lett.* **90**, 052501 (2003).
  - [15] L. El Fassi *et al.*, *Phys. Lett. B* **712**, 326 (2012).
  - [16] Nuruzzaman *et al.*, *Phys. Rev. C* **84**, 015201 (2011).
  - [17] S. Das, *Phys. Rev. C* **100**, 035203 (2019).
  - [18] <http://pdg.lbl.gov/xsect/contents.html>; S. Navas *et al.* (Particle Data Group), *Phys. Rev. D* **110**, 030001 (2024), <http://pdf.lbl.gov>.
  - [19] T. H. Bauer, R. D. Spital, D. R. Yennie, and F. M. Pipkin, *Rev. Mod. Phys.* **50**, 261 (1978).
  - [20] D. R. Yennie, *Hadronic Interactions of Electrons and Photons: Proceedings of the 11th Session of the Scottish Universities Summer School in Physics, 1970*, edited by J. Cumming and H. Osborn (Academic, New York, 1971), p. 321.
  - [21] J. Hüfner, B. Kopeliovich, and J. Nemchik, arXiv:hep-ph/9511215; Invited talk given by B. Kopeliovich at the ELFE Workshop, Cambridge, 22-29 July, 1995.
  - [22] A. Sibirtsev, H.-W. Hammer, U.-G. Meißner, and A. W. Thomas, *Eur. Phys. J. A* **29**, 209 (2006).
  - [23] S. Das, *Phys. Rev. C* **103**, 035205 (2021); *Proc. Nucl. Phys.* **63** 828 (2018).
  - [24] Ph. Gubler, M. Ichikawa, T. Song, and E. Bratkovskaya, arXiv:2408.15364v1 [hep-ph].
  - [25] S. D. Drell and J. S. Trefil, *Phys. Rev. Lett.* **16**, 552 (1966).
  - [26] A. B. Larionov, M. Strikman and M. Bleicher, *Phys. Rev. C* **93**, 034618 (2016).
  - [27] D. Dutta *et al.*, *The Search for Color Transparency at 12 GeV*, Jefferson Lab experiment E12-06-107, 2006 (unpublished).
  - [28] W. Cosyn, M. C. Marti'nez and J. Ryckebusch, *Phys. Rev. C* **77**, 034602 (2008).
  - [29] G. R. Farrar, H. Liu, L. L. Frankfurt and M. I. Strikman, *Phys. Rev. Lett.* **61**, 686 (1988).
  - [30] S. R. Amendolia *et al.*, *Phys. Lett. B* **178**, 435 (1986).
  - [31] A. S. Carroll *et al.*, *Phys. Lett. B* **80**, 319 (1979).